Biomaterials 85 (2016) 204–217

Contents lists available at ScienceDirect

Biomaterials

journal homepage: www.elsevier.com/locate/biomaterials

Synthesis and characterization of anti-bacterial and anti-fungal citrate-based mussel-inspired bioadhesives

Jinshan Guo [a, 1], Wei Wang [a, b, 1], Jianqing Hu [a, c, 1], Denghui Xie [d], Ethan Gerhard [a], Merisa Nisic [a], Dingying Shan [a], Guoying Qian [b], Siyang Zheng [a], Jian Yang [a, *]

[a] Department of Biomedical Engineering, Materials Research Institute, The Huck Institutes of the Life Sciences, The Pennsylvania State University, University Park, PA 16802, USA
[b] Zhejiang Provincial Top Key Discipline of Bioengineering, College of Biological and Environmental Sciences, Zhejiang Wanli University, Ningbo 315100, China
[c] School of Chemistry and Chemical Engineering, South China University of Technology, Guangzhou 510640, China
[d] Department of Orthopedic Surgery, The Third Affiliated Hospital of Southern Medical University, Academy of Orthopedics of Guangdong Province, Guangzhou 510630, China

ARTICLE INFO

Article history:
Received 16 December 2015
Received in revised form
27 January 2016
Accepted 31 January 2016
Available online 2 February 2016

Keywords:
Wound closure
Antibacterial
Antifungal
Citric acid
Sodium metaperiodate
Silver nanoparticles

ABSTRACT

Bacterial and fungal infections in the use of surgical devices and medical implants remain a major concern. Traditional bioadhesives fail to incorporate anti-microbial properties, necessitating additional anti-microbial drug injection. Herein, by the introduction of the clinically used and inexpensive anti-fungal agent, 10-undecylenic acid (UA), into our recently developed injectable citrate-based mussel-inspired bioadhesives (iCMBAs), a new family of anti-bacterial and anti-fungal iCMBAs (AbAf iCs) was developed. AbAf iCs not only showed strong wet tissue adhesion strength, but also exhibited excellent *in vitro* cyto-compatibility, fast degradation, and strong initial and considerable long-term anti-bacterial and anti-fungal ability. For the first time, the biocompatibility and anti-microbial ability of sodium metaperiodate (PI), an oxidant used as a cross-linking initiator in the AbAf iCs system, was also thoroughly investigated. Our results suggest that the PI-based bioadhesives showed better anti-microbial properties compared to the unstable silver-based bioadhesive materials. In conclusion, AbAf iCs family can serve as excellent anti-bacterial and anti-fungal bioadhesive candidates for tissue/wound closure, wound dressing, and bone regeneration, especially when bacterial or fungal infections are a major concern.

1. Introduction

The clinical applications of biomaterials with adhesive properties as wound closure or hemostatic agents, tissue sealants, and wound dressings have advanced surgeries in terms of the facilitation of surgical operations, the improvement of patient compliance, and the reduction of healthcare costs by reducing the use of sutures, medical gauze, and other auxiliary materials [1–3]. Bacterial and fungal infections are major concerns in the use of surgical devices or implants for wound closure and wound repair, which result in prolonged wound healing, wound dehiscence, abscess formation and even sepsis, especially for applications in large area burn wound repair, wound closure for patients suffering from diabetes or other immune compromising diseases, and wound care in infection prone areas such as diabetic foot ulcers [1,4–7]. Treatment of localized fungal infections, such as osteoarticular infections, can be extremely difficult, because they take on an abscess-like or granulomatous form and relatively sequestered from circulating drugs [7]. Traditional bioadhesives typically lack native anti-bacterial and anti-fungal properties, necessitating additional anti-bacterial and anti-fungal drug injection. The inconvenience of these repeated injections and the resulting increase in cost as well as the toxicity concerns continues to limit the potential of current bioadhesives. Even if anti-microbial drugs are encapsulated in bioadhesives, sustained release is difficult to achieve and the burst release of drugs often results in undesired systemic toxicity. The development of biocompatible bioadhesives

* Corresponding author. W340 Millennium Science Complex, University Park, PA 16802, USA.
E-mail address: jxy30@psu.edu (J. Yang).
[1] These authors contribute equally to this work.

http://dx.doi.org/10.1016/j.biomaterials.2016.01.069
0142-9612/

with intrinsic anti-bacterial and anti-fungal properties for local application in tissue/wound closure, wound dressing, or bone regeneration is urgently needed.

Biodegradable citrate-based polymers, benefitting from facile synthesis reaction and modification, excellent processing possibilities, and tailored mechanical and degradation properties, were developed in our lab for cardiovascular and orthopedic applications, as well as applications in bioimaging, drug/cell delivery, and bioadhesives [8–18]. The development of injectable citrate-based mussel-inspired bioadhesives (iCMBA) fully utilized the facile reactivity of citric acid to modify our citrate-based polymer with dopamine, a derivative of L-3, 4-dihydroxyphenylalanine (L-DOPA) that contributes to the strong under-water adhesive properties of marine mussels [19,20], through a convenient one-pot polycondensation process [18]. Citric acid is a naturally-derived organic compound that abundantly exists in citrus fruits, such as lemons and limes. As an important intermediate in the Krebs cycle that occurs in the metabolism of all aerobic organisms, citric acid is nontoxic and biocompatible [8]. As a weak organic acid, citric acid is also a natural preservative and flavoring agent used in the food industry [21]. The anti-bacterial ability of citrate-based polymers developed in our lab was also recently testified, which was attributed to that the abundant free carboxyl groups derived from citrates in the polymers may lower the local pH, suppress the nicotinamide adenine dinucleotide (NADH) oxidation, and/or chelate the metal ions in the cell wall thus altering the permeability of cell wall for nutrient uptakes to cause cell damage and then death [22].

Although citrate-based polymers possess an intrinsic anti-bacterial ability, it might be insufficient to combat wound infection without additional anti-bacterial additives. Silver and silver ions, especially silver nanoparticles that have relatively large surface areas to contact with bacteria or fungi, have been widely studied and utilized as effective anti-microbial agents [6,23,25]. Polymers containing catechol groups (from dopamine) have the ability to transform silver nitrate into silver nanoparticles by oxidation–reduction reaction and can be used for anti-bacterial purposes, as proven by previous studies [25]. Additionally, water-soluble oxidants such as sodium (meta) periodate (PI), used in our iCMBA cross-linking process, have been commonly used as anti-microbial agents in aquaculture.

In the present work, 10-undecylenic acid (UA), used as an anti-fungal agent against *Panneuritis epidemica*, was conjugated to citric acid to create a new anti-fungal citric acid (U-CA, Scheme 1A). Through a convenient one-pot polycondensation reaction of citric acid, anti-fungal citric acid (U-CA), L-dopamine, and hydrophilic poly (ethylene glycol) (PEG), a water soluble anti-fungal iCMBA pre-polymers (AiCs) were obtained. The cross-linking of AiCs was conducted by the addition of silver nitrate or sodium (meta) periodate (PI), which led to dual-functional anti-bacterial and anti-fungal iCMBA bioadhesives (AbAf iCs). The cytocompatibility of these bioadhesives was studied against human-derived mesenchymal stem cells (hMSCs). The short-term and long-term anti-bacterial and anti-fungal performances of these AbAf iCs were also thoroughly investigated using two kinds of bacteria, *Staphylococcus aureus* (*S. aureus,* from ATCC) as a representative Gram-positive bacteria and *Escherichia coli* (*E. coli,* from ATCC) as a representative Gram-negative bacteria, and *Candida albicans* (*C. albicans*) as a representative fungi that is often found in diabetic foot infections.

2. Experimental section

2.1. Materials

All chemicals were purchased from Sigma–Aldrich and used without further purification, except where mentioned otherwise.

2.2. General measurements

^{1}H-NMR spectra of monomer and pre-polymers in DMSO-d_6 were recorded on a 300 MHz Bruker DPX-300 FT-NMR spectrometer. Fourier transform infrared (FTIR) spectra were measured with a Nicolet 6700 FTIR spectrometer. Sample solutions in acetone were cast onto KBr plates, with blank KBr used as background. UV–vis spectra were recorded using a UV-2450 spectrometer (Shimadzu, Japan) with a minimum wavelength resolution of 0.2 nm.

2.3. Polymer syntheses

2.3.1. Anti-fungal citric acid monomer (U-CA) synthesis

A new anti-fungal citric acid monomer was synthesized by modifying citric acid (CA) with 10-undecylenic acid (UA) via a method similarly described elsewhere (Scheme 1A) [26]. Briefly, citric acid (9.606 g, 0.05 mol) and zinc chloride ($ZnCl_2$, 0.6815 g, 0.005 mol, 0.1 eq. to CA) were added into 10-undecenoyl chloride (21.5 mL, 0.1 mol) in a dried 100-mL round-bottom flask. The reaction mixture was heated at 90 °C with stirring for 24 h. After cooling down to room temperature, diethyl ether (100 mL) was added to the mixture, and the solution was poured into ice water (50 mL) with stirring. The organic portion was separated, dried over anhydrous sodium sulfate, and the solvent was then evaporated. The crude product was purified by precipitation in hexane (250 mL). The product, 10-undecylenic acid modified citric acid (U-CA), was obtained as viscous dark brown oil (12.7 g, 71% yield). ^{1}H NMR (300 MHz; DMSO-*d6*; δ, ppm) of U-CA: 1.25–1.35 (s, $OCOCH_2CH_2-(C\mathbf{H}_2)_5-$ from UA), 1.52 (s, $OCOCH_2C\mathbf{H}_2-$ from UA), 1.98–2.05 (m, $CH_2{=}CH{-}C\mathbf{H}_2-$ from UA), 2.25–2.30 (m, $OCOC\mathbf{H}_2-$ from UA), 2.65–3.00 (m, $-C\mathbf{H}_2-$ from CA), 4.91–5.02 (m, $C\mathbf{H}_2{=}$ CH– from UA), 5.74–5.84 (m, $CH_2{=}C\mathbf{H}-$ from UA). FTIR of U-CA (cast film on KBr, cm^{-1}): 1897 ($-\underline{CH_2}-$) and 1733 ($\underline{COO}R$).

2.3.2. Anti-fungal iCMBA pre-polymers (AiCs) synthesis and characterization

Anti-fungal iCMBA (AiC) pre-polymers were synthesized by polycondensation of citric acid (CA), U-CA, poly(ethylene glycol) (PEG), and catechol-containing compounds, such as dopamine and L-DOPA (L-3,4-dihydroxyphenylalanine), as illustrated in Scheme 1B, adapting a method used in our previous work [18]. Briefly, CA (17.29 g, 0.09 mol), U-CA (7.18 g, 0.02 mol) and PEG200 (with an average molecular weight of 200Da, 20 g, 0.10 mol) were placed in a 100-mL round-bottom flask and heated to 160 °C until a molten, clear mixture was formed under stirring. Then the temperature was reduced to 140 °C, followed by the addition of dopamine (5.69 g, 0.03 mol) under N_2 atmosphere. The reaction was continued under vacuum for approximately 6 h until the stir bar twitched at 60 rpm. Then the reaction was stopped and the pre-polymer was dissolved in deionized (DI) water and purified by extensive dialysis using a dialysis tube with a molecular weight cut-off (MWCO) of 500 Da. After freeze-drying of the dialyzed solution, AiC-P_{200} pre-polymer was obtained. By adjusting the molecular weight and architectural structure (linear or branched) of PEG used, different AiC pre-polymers were synthesized as shown in Table 1. The feeding amount of dopamine was fixed at the ratio of 1.1/0.3 ((CA+U-CA)/dopamine). FTIR of AiC (Fig. 1A, by casting polymer solution in acetone on KBr, cm^{-1}): 1898 ($-\underline{CH_2}-$) and 1734 ($\underline{COO}$-), 1633 ($\underline{CO}NH-$). Representative ^{1}H NMR (Fig. 1B, 300 MHz; DMSO-d_6; δ, ppm) of AiC pre-polymer: 1.22 (s, $OCOCH_2CH_2-(C\mathbf{H}_2)_5-$ from UA), 1.47 (s, $OCOCH_2C\mathbf{H}_2-$ from UA), 1.65 (m, $CH_2{=}CH{-}C\mathbf{H}_2-$ from UA), 2.25–2.30 (m, $OCOC\mathbf{H}_2-$ from UA), 2.65, 3.05 (m, $-C\mathbf{H}_2-$ from CA and citric acid of U-CA), 4.77 (broad, $C\mathbf{H}_2{=}$CH– from UA), 5.34

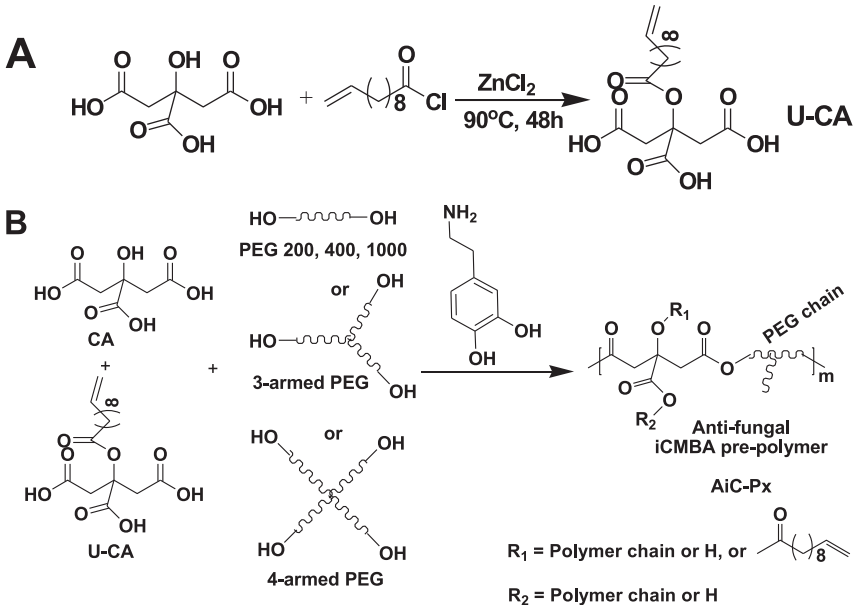

Scheme 1. Synthesis of anti-fungal citric acid (undecylenate citric acid, U-CA) monomer and anti-fungal injectable citrate-based mussel-inspired bioadhesives pre-polymer (anti-fungal iCMBA pre-polymer, AiC).

Table 1
Nomenclature, feeding ratio and dopamine content of pre-polymers.

Pre-polymer name	Mw of PEG used (Da)	Feeding ratio of CA: U-CA: PEG: Dopamine	Dopamine content in pre-polymer (mmol/g)
iC-P_{200}	200	1.1: 0: 1: 0.3	0.756
AiC-P_{200}	200	0.9: 0.2: 1: 0.3	0.669
AiC-P_{400}	400	0.8: 0.3: 1: 0.3	0.470
AiC-$P_{2/4\ (1/1)}$ (PEG 200 and 400, w/w = 1/1)	200 & 400	0.8: 0.3: 1: 0.3	0.538
AiC-P_{1000}	1000	0.8: 0.3: 1: 0.3	0.273
AiC-P_{3A1000}	1000 (3 armed)	0.8: 0.3: 0.667: 0.3	0.225
AiC-P_{4A800}	797 (4 armed)	0.8: 0.3: 0.5: 0.3	0.258

(broad, CH_2=C**H**– from UA).

The dopamine content in AiCs was also determined by UV–vis spectra, where absorbance of 0.4 mg/mL solution of various pre-polymers in DI water were measured using Shimadzu UV-2450 spectrophotometer across the wavelength of 700–200 nm.

2.4. Cross-linking of AiC and setting time measurement

Two different kinds of oxidants, silver nitrate ($AgNO_3$, SN for short) and sodium (meta) periodate (PI), were used to cross-link AiC into anti-bacterial and anti-fungal iCMBAs (AbAf iCs).

The cross-linking of AiC by SN was conducted as similar to a previously described method [25]. The effect of pH value of iCMBA pre-polymer solution on the setting time was investigated using a representative polymer, iC-P_{200} (iCMBA formed by PEG200 without using U-CA, with a dopamine feeding ratio of 0.3 to PEG). The optimal pH value obtained by this study was 8.5, which agrees with the literature [25]. Thus the cross-linking of AiC by SN was conducted at pH 8.5. Briefly, AiCs were dissolved in Tris-HNO_3 buffer solution (pH 13) with a concentration of 50 wt%, and the pH value was adjusted to 8.5. Then SN solution in Tris-HNO_3 buffer (pH 8.5) (for 1 g of pre-polymer, use 1 mL of SN solution) was added into AiC solution. Oxidation and consequently the cross-linking reaction of catechol-containing AiC were triggered upon mixing. Gelation or setting time of AiC was measured by a viscometry technique as described in our previous work [18]. The cross-linking of AiCs by PI was conducted as reported previously [18].

2.5. Properties of cross-linked anti-bacterial and anti-fungal iCMBAs (AbAf iCs)

Mechanical properties of dried cross-linked AbAf iCs, including tensile strength, Young's modulus and elongation at break, were measured according to ASTM D412A on an Instron 5966 machine fitted with a 10 N load cell (Instron, Norwood, MA). Briefly, dog bone shaped samples (25 mm × 6 mm × 1.5 mm, length × width × thickness) were pulled at a rate of 500 mm/min and elongated to failure. The Young's modulus was obtained by calculating the gradient from 0 to 10% of elongation of the stress–strain curve. Eight specimens per sample were tested and averaged. In order to evaluate the effect of hydration on the mechanical properties, the mechanical tests were also conducted on fully swollen samples after being hydrated and swollen in water for 4 h.

The sol/gel content, an indication of non-crosslinked/crosslinked fractions of the hydrogel, and swelling ratio were measured by the mass differential before and after incubation of the cross-linked polymer in 1, 4-dioxane (sol content) or water (swelling ratio) as described previously [18]. The sol content (Fig. 3C) and swelling ratio (Fig. 3D) were then calculated using equations (1) and (2), respectively.

$$\text{Sol content } (\%) = \frac{W_i - W_d}{W_i} \times 100 \quad (1)$$

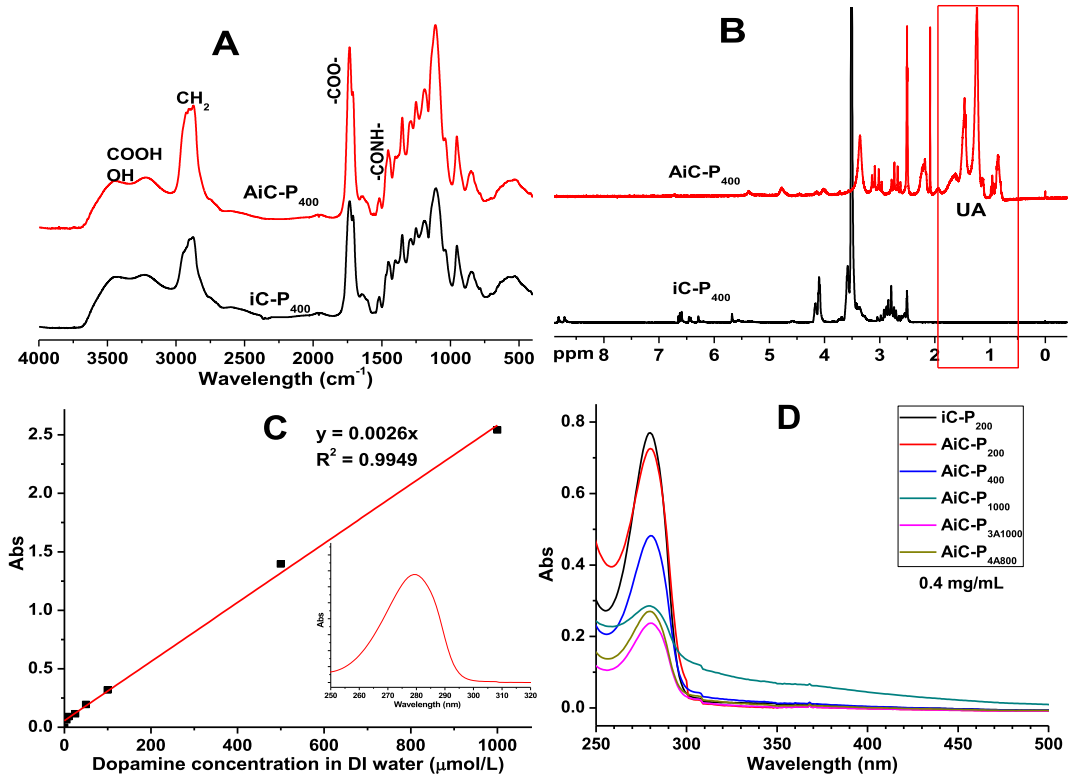

Fig. 1. Characterization of pre-polymers: FTIR (A) and ^{1}H-NMR (B) spectra of iCMBA (iC-P_{400}) and anti-fungal iCMBA (AiC-P_{400}); (C) Standard curve of dopamine in DI water (insert figure is the representative UV–vis absorption spectrum) and (D) UV–vis absorption spectra of iCMBA and anti-iCMBA pre-polymers (with a pre-polymer concentration of 0.4 mg/mL).

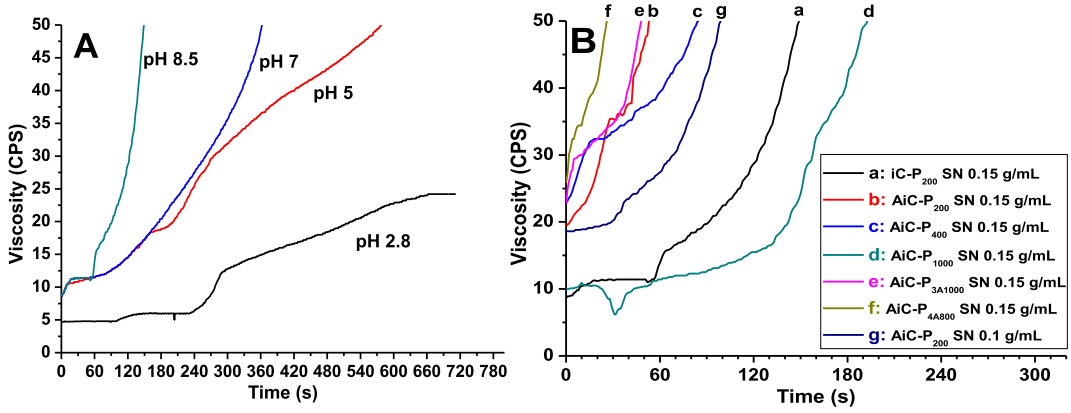

Fig. 2. Gelling time test: Viscosity-time curves of iC-P_{200} cross-linked with 0.15 g/mL silver nitrate (SN) at different pH (A) and different iCMBA and anti-fungal iCMBA pre-polymers crosslinked with various SN concentrations at pH 8.5 (B).

$$\text{Swelling ratio } (\%) = \frac{W_s - W_d}{W_d} \times 100 \quad (2)$$

Here W_i represents the initial dry weight of cross-linked hydrogel disk, W_d represents the weight of freeze-dried sample after the uncross-linked part was washed by 1, 4-dioxane for 48 h, and W_s represents the network weight after the leached and dried sample was suspended in water for 24 h.

Degradation studies were conducted in PBS (pH 7.4) and at 37 °C using cylindrical disc specimens (7 mm in diameter, 2 mm thick) as described previously [15]. The mass loss was calculated by comparing the initial mass (W_0) with the mass measured at the pre-determined time points (W_t) using equation (3).

$$\text{Mass loss } (\%) = \frac{W_0 - W_t}{W_0} \times 100 \quad (3)$$

2.6. Adhesion strength of AbAf iCs

The adhesion strength of AbAf iCs cross-linked by SN or PI was determined by the lap shear strength test according to the modified ASTM D1002-05 method as described in our previous study [18]. The results are shown in Fig. 4.

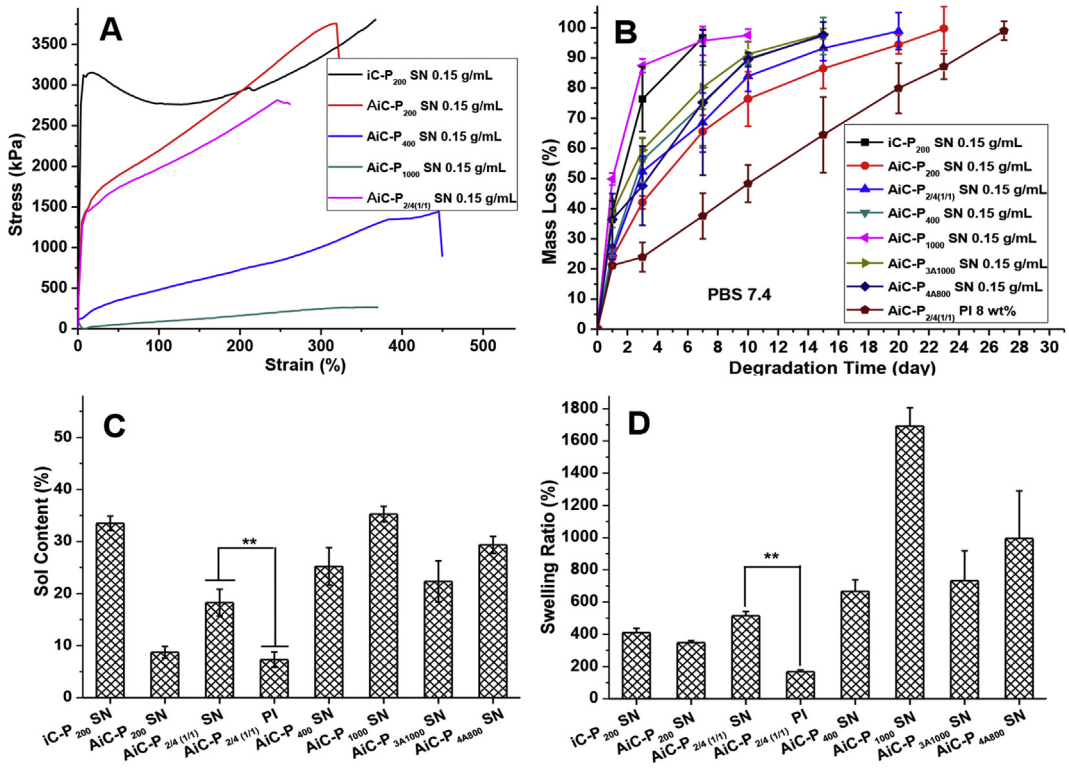

Fig. 3. Physical and degradation properties: Mechanical properties (stress–strain curves (A), degradation profiles (B), Leachable parts (sol content) (C), and swelling ratios (D) of anti-bacterial anti-fungal injectable citrate-based mussel-inspired bioadhesives (AbAf iCs) cross-linked by silver nitrate (SN) or sodium periodate (PI).

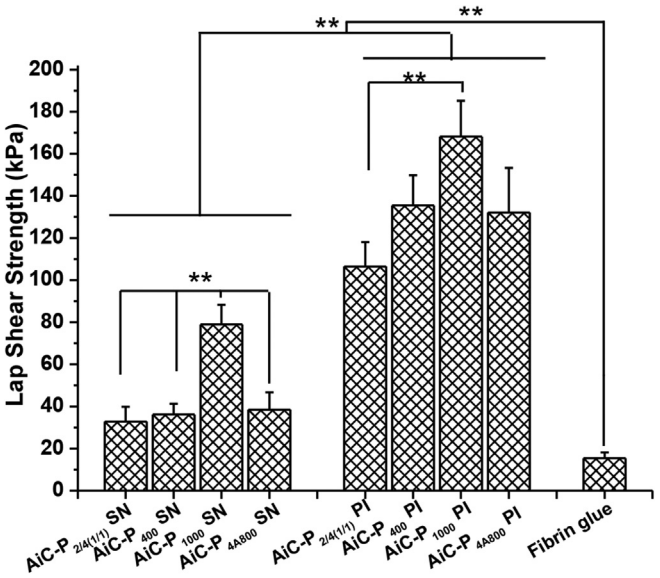

Fig. 4. Adhesion strength of AbAf iCs cross-linked by silver nitrate (SN) or sodium periodate (PI) and fibrin glue to wet porcine small intestine submucosa measured by lap shear strength tests (**$p < 0.01$).

2.7. Cytocompatibility tests of AiC pre-polymers and cross-linked AbAf iC hydrogels

Human-derived mesenchymal stem cells (hMSCs, ATCC® PCS-500-012TM) were purchased from ATCC, and passages 5–10 were used for cytotoxicity study in this work. *In vitro* pre-polymer cytotoxicity was assessed by MTT (methylthiazolyl -diphenyl-tetrazolium bromide) assay against hMSCs. First, different AiC pre-polymers were dissolved into complete Dulbecco's modified eagle's medium (DMEM, with 10% (v/v) fetal bovine serum (FBS) and 1% (v/v) antibiotic antimycotic solution (100 ×)), namely growth media (MG), with a pre-polymer concentration of 10 mg/mL, and the pH value of the solutions was adjusted to 7.4 before use. Then the 10 mg/mL pre-polymer solutions in MG were diluted 10 and 100 times by blank MG media to make a pre-polymer containing MG solution with a final concentration of 1 and 0.1 mg/mL respectively. Next, to each well of a 96-well cell culture plate, 200 μL of hMSC solution in MG, with a density of 5×10^4 cells/mL, was added and incubated for 24 h at 37 °C, 5% CO_2 and 95% relative humidity. Twenty four hours post cell seeding, the medium was completely replaced by 200 μL of pre-polymer containing MG media with various concentrations (10, 1, and 0.1 mg/mL), and incubated for another 24 h followed by MTT assay. Poly (ethylene glycol) diacrylate (PEGDA, M_n = 700Da) solutions with the same weight concentrations were used as negative controls as previously described [18]. Viabilities of cells in pre-polymer or PEGDA containing MG media were normalized to that of cells cultured in blank MG media. Cytotoxicity of CA and PI with different concentrations was also assessed using the same method.

The cytotoxicity of sol contents (or leachable fractions) and degradation products of AbAf iC hydrogels, cross-linked by SN or PI, were also studied using MTT assay against hMSCs, with iC-P_{200} PI 8 wt%, synthesized according our previous study as a control [18]. The sol content solution of AbAf iC hydrogel was obtained by incubating equal mass (0.5 g) hydrogel specimens in 5 mLs of PBS (pH 7.4) at 37 °C for 24 h. Next, three different solutions were prepared: 1 × , 10 × and 100 × (1 × was the solution of leached products with no dilution; 10 × and 100 × means 10 times and 100 times dilution of 1 × solution by PBS, respectively). To each well of a 96-well cell culture plate, 200 μL of hMSC solution in MG medium

with a density of 5×10^4 cells/mL was added and incubated for 24 h. Then, 20 μL of sol content solutions with various concentrations were added and the cells were incubated for another 24 h followed by MTT assay.

The cytotoxicity of degradation products of AbAf iC hydrogels was also evaluated. Equal weight (1 g) of AbAf iC hydrogel samples as well as poly (lactic-co-glycolic acid) (PLGA, used as control, LA/GA = 50/50, Mw~60 KDa, purchased from Polyscitech) were fully degraded in 10 mL of 0.2 M NaOH solution. After adjusting pH value to 7.4, the resultant solutions were diluted to three concentrations (1 ×, 10 × and 100 ×) using PBS (pH 7.4), and used for cell culture (the process was the same as that used in sol content cell cytotoxicity study described above) and subsequent MTT analysis.

All the above solutions were pH-neutralized and passed through a sterilized 0.2 μm filter prior to use for cell culture. The cell viability results were normalized to the viability of cells in blank MG medium.

Cell adhesion and proliferation on cross-linked AbAf iC films was also studied against hMSC cells. The morphology of hMSC cells was observed by Live/Dead staining assay. Briefly, about 20 μL of AbAf iC mixture (containing AiC pre-polymer and oxidant, SN or PI) (prior to completion of cross-linking) was uniformly spread on the surface of a glass slide with a diameter of 15 mm to form a thin layer of the cross-linked AbAf iC. The samples were then sterilized by incubation in 70% ethanol for 24 h followed by exposure to UV light for 3 h. The samples were then placed in 24-well plates and seeded with 500 μL hMSC solutions with a density of 5000 cells/cm^2 followed by MG media replacement the next day. At each time point (1, 3 and 7 days post cell seeding), the constructs were removed from the well plate, rinsed by PBS, and stained by Live/Dead Viability/Cytotoxicity Kit (Invitrogen, molecular probes, Eugene, OR) for the observation of cell morphology using an inverted light microscope (Nikon Eclipse Ti–U) equipped with a ANDOR DL-604M-#VP camera and Prior Lumen 200. The results are shown in Fig. 5D.

2.8. Anti-bacterial performance of AbAf iC bioadhesives

2.8.1. Bacterial incubation

Staphylococcus aureus (*S. aureus*, ATCC® 6538™) and *Escherichia coli* (*E. coli*, ATCC® 25922™) were purchased from ATCC (American Type Culture Collection) and used following established safety protocols. Tryptic soy broth (Cat. #: C7141) and tryptic soy agar (Cat. #: C7121) used for *S. aureus* culture were purchased from Criterion (through VWR). Luria broth base (LB broth, Cat. #: 12795-027) and select agar (Cat. #: 30391-023) used for *E. coli* culture were purchased from Invitrogen. *S. aureus* and *E. coli* were cultivated at 37 °C in sterilized tryptic soy broth and LB broth respectively with a speed of 150 rpm in a rotary shaker overnight and the obtained bacteria suspensions were diluted into various concentrations before use.

2.8.2. Bacterial inhibition kinetics curves

To examine the kinetics of bacterial growth and the inhibition ratio of AbAf iC hydrogels cross-linked by SN or PI, AiC-$P_{2/4(1/1)}$ SN 0.15 g/mL (AiC-SN) and AiC-$P_{2/4(1/1)}$ PI 8wt% (AiC-PI) were chosen as the representative experimental groups, and iC-P_{200} PI 8 wt% (iC-PI) and PEGDA/HEMA hydrogels (M_n of PEGDA is 700Da, w/w between PEGDA and 2-Hydroxyethyl methacrylate (HEMA) = 1/1, cross-linked by APS and TEMED) [27] were used as controls. Citric acid (29 mg/mL) and PI (8 wt%) solutions were also tested. The bacterial inhibition kinetics to both *S. aureus* and *E. coli* were tested. For each hydrogel sample, 0.2 g of freeze-dried hydrogel was immersed in 20 mL of germ containing nutrient solution with a bacterial concentration of optical density (OD) at 600 nm around 0.1. Incubation was performed at 37 °C with an orbital shaker with a speed of 150 rpm for 24 h. Pure growth broth without bacterials was also tested and served as a control. The bacterial broth medium was taken out at pre-set intervals (200 μL each time), and the OD value of the medium at 600 nm was recorded by a microreader (TECAN, infinite M200 PRO). The inhibition ratios of hydrogels or other supplements (CA or PI) were calculated by equation (4):

$$\text{Inhibition ratio}(\%) = 100 - 100 \times \frac{A_t - A_0}{A_{con} - A_0} \quad (4)$$

Where A_0 was the OD value of bacterial broth medium before incubation, and A_t and A_{con} were the OD values of hydrogel/supplement-containing medium and pure medium (control) after incubation for the designated time, respectively.

2.8.3. Zone of inhibition against bacteria test

AiC-SN, AiC-PI, and iC-PI, as well as PEGDA/HEMA hydrogel, were used to test anti-bacterial inhibition halos by modified Kirby Bauer technique [6,21]. Briefly, 10 mL of bacteria medium (with an OD value at 600 nm around 0.1, both *S. aureus* and *E. coli* were tested) was dispersed onto a tryptic soy/LB agar plate (Φ140 × 7 mm). Then Hydrogel disks (around Φ5 × 3 mm) were placed on the agar plate and incubated for 24 h at 37 °C. After incubation, the bacterial inhibition halos around the hydrogel samples were observed and their diameters were measured.

2.8.4. Minimal inhibitory concentration (MIC) tests of CA, UA, and PI against bacteria

The minimal inhibitory concentrations (MICs) of citric acid (CA), buffered CA (pH 7.4), 10-undecylenic acid (UA), and PI against *S. aureus* and *E. coli* were measured using the broth macrodilution method (using 2 × gradient dilution) [28]. Bacteria were incubated at 37 °C for 24 h. Bacterial survival ratios were calculated by equation (4), and the MICs were determined as the lowest drug concentrations that induced complete inhibition of bacteria growth.

2.8.5. Anti-bacterial properties of degradation products and release solutions of AbAf iC bioadhesives

To evaluate the long-term effect of AbAf iC hydrogels on bacteria, the anti-bacterial properties of degradation products and periodical release solutions of AbAf iC hydrogels were tested, using iC-PI and PEGDA/HEMA as controls.

For the anti-bacterial evaluation of degradation products, 1 g of freeze-dried hydrogel was fully degraded in 10 mL 0.2 M NaOH solution, and then diluted into 1 ×, 10 × and 100 × solutions after adjusting the pH to 7.4 and sterilization by filtering through a 0.2 μm filter (1 × means no dilution, 10 × and 100 × means being diluted 10 and 100 times respectively by tryptic soy broth/LB broth). For the bacteria inhibition ratio test, degradation product solutions (with various dilutions) were added in the wells of 24-well plates with 450 μL per well. 50 μL of bacteria suspension was added into each well to give initial bacteria concentration of OD_{600nm} around 0.1. Control samples were established by diluting 50 μL of the same bacteria suspension in 450 μL of blank broth medium. The 24-well plates were incubated at 37 °C for 24 h with a shaking speed of 150 rpm followed by OD value recording. The bacteria inhibition ratio was calculated by equation (4).

For release solution anti-bacterial evaluation, 0.1 g freeze-dried hydrogel was placed into a sterilized 15-mL centrifuge tube after being sterilized by UV for 30 min, and 5 mLs of tryptic soy broth or LB broth was added to the tube. The hydrogel suspension was shaken at 37 °C, and the periodical release solutions were collected after shaking for 4, 8, and 14 days (broth medium was totally

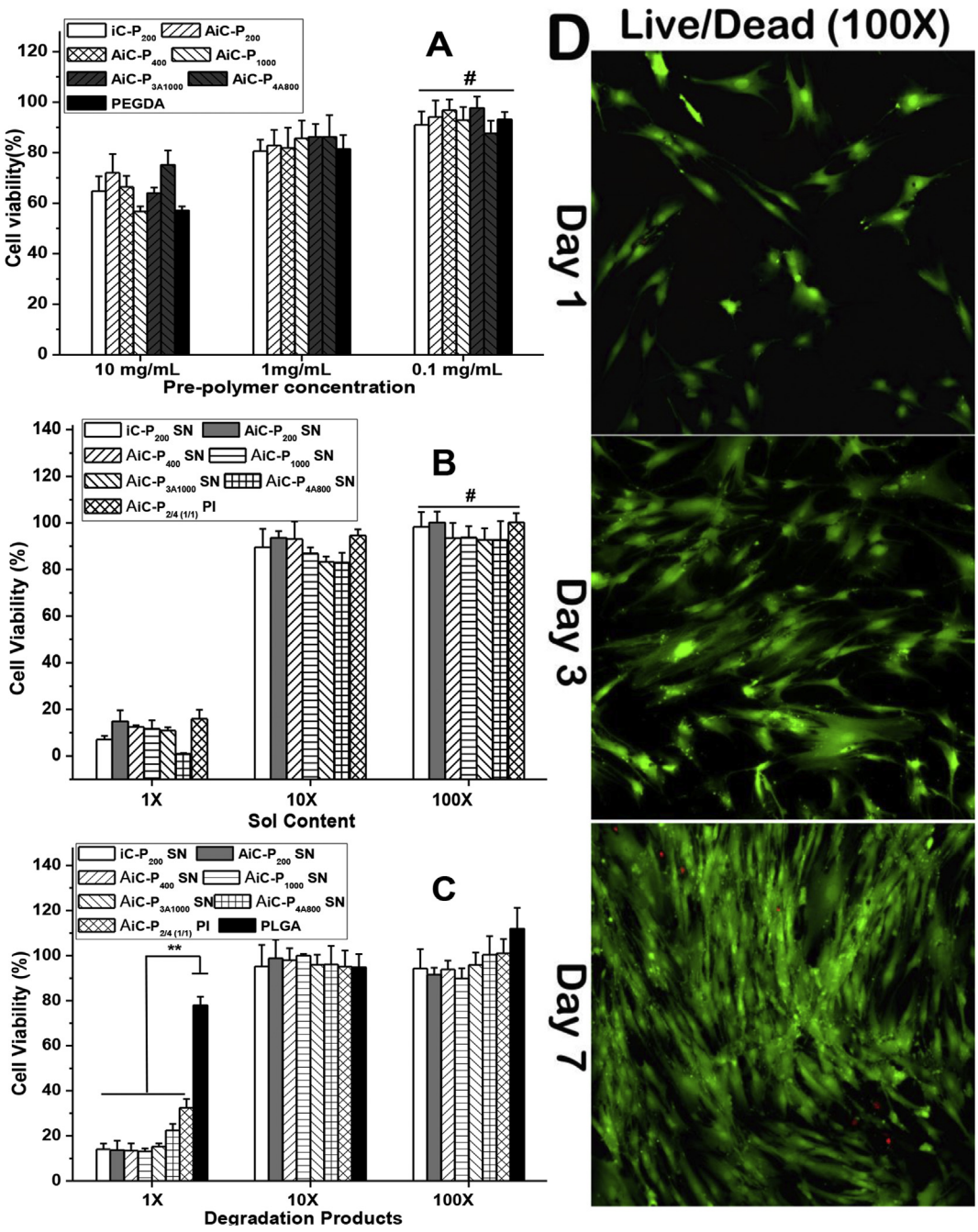

Fig. 5. Cytotoxicity evaluation of anti-bacterial and anti-fungal iCMBAs (AbAf iCs) against human-derived mesenchymal stem cells (hMSC) by MTT assay. (A) anti-fungal iCMBA pre-polymers, (B) leachable part (sol content), (C) degradation product, (D) Cell morphology on AbAf iCMBA films by Live/Dead staining at 1st, 3rd, and 7th day post-seeding.

replaced at each time point). The bacteria inhibition ratios of these periodical release solutions were measured using the same method described in the bacterial inhibition ratio test of degradation products.

2.9. Anti-fungal performance of AbAf iC bioadhesives

2.9.1. Fungi incubation

Fungi (*Candida albicans*, *C. albicans*, ATCC® 10231™) was used following established safety protocols. YM medium broth (Lot #: 1964C030) and YM agar (Lot #: 1964C030) used for fungi (*C. albicans*) culture were obtained from Amresco and Acumedia separately through VWR. Tween 20 was added to YM broth medium with a final concentration of 0.5wt% and sterilized before being used for fungi culture in broth (the addition of Tween 20 can stabilize the suspension of fungi in YM broth). In all cases, *C. albicans* was maintained on YM agar plates. For experiments, *C. albicans* was scraped from YM agar plates and dispersed in Tween 20 containing YM broth medium, counted with a hemocytometer, and diluted into a final fungi concentration of $0.5–1 \times 10^7$ cells/mL [7]. The actual measure of fungal survival used a colony growth assay on YM agar plates is described in detail below.

2.9.2. Anti-fungal effect of direct exposure to hydrogels

The anti-fungal effect of direct exposure to AbAf iC hydrogels was tested using AiC-SN and AiC-PI as representative experimental groups, and iC-PI and PEGDA/HEMA hydrogels as controls. Briefly, 10 mg freeze-dried hydrogel disks were placed in the wells of a 24-well tissue culture plate, and 1 mL of *C. albicans* suspension in Tween-20 containing YM broth medium ($0.5–1 \times 10^7$ cells/mL) was added to each well. Samples without hydrogel were used as blank controls. The 24-well plates were incubated for 3 h at 37 °C with shaking speed of 100 rpm. Then the hydrogel disks were removed, the remaining medium was diluted 300 times, and 0.3 mL diluted medium was removed and cast on YM agar plates (Φ6 × 2 mm). After incubation at 37 °C for 24 h, fungi colonies on the YM agar plates were counted, and the fungi survival ratios were calculated according to equation (5). For each sample, at least 6 plates were cast, and the numbers were averaged.

$$\text{Fungal survival ratio } (\%) = \frac{N_s}{N_{con}} \times 100 \quad (5)$$

Here, N_s stands for the number of fungal colonies for samples, and N_{con} stands for the number of fungal colonies for YM broth blank control.

2.9.3. Halo test

The anti-fungal performance of AiC-SN and AiC-PI was also tested by the halo test method using iC-PI and PEGDA/HEMA hydrogels as controls. Briefly, 4 mLs of YM broth medium containing $0.5–1 \times 10^7$ cells/mL *C. albicans* was evenly cast onto YM agar plates (Φ85 × 6 mm). The hydrogel discs (around Φ5 × 3 mm) were placed on the agar plate and the constructs were incubated at 37 °C for 24 h in the dark before being examined for a "halo" or "zone of inhibition" surrounding the gel disc.

2.9.4. Minimal inhibitory concentrations (MICs) tests of CA, UA, and PI against fungi

The MICs of CA, buffered CA (pH 7.4), UA, PI, and AiC-$P_{2/4(1/1)}$ as well as iC-P_{200} pre-polymers to *C. albicans* were measured using the agar dilution method (using 2 × gradient dilution) [24]. CA or other samples in YM agar with various concentrations were injected into the wells of 6-well tissue culture plates when the hot YM agar solution was still flowable (3 mL each well). After solidification, fungi suspension in YM broth ($0.5–1 \times 10^5$) was spread onto YM agar (0.3 mLs each well), and the plates were incubated at 37 °C for 24 h. The fungi survival ratios were calculated by equation (5), and the MICs were determined as the lowest drug concentrations that induced complete inhibition of fungi growth.

2.9.5. Anti-fungal properties of degradation products and release solutions of AbAf iC bioadhesives

The anti-fungal properties of degradation products and periodical release solutions of AbAf iCs were tested using AiC-SN and AiC-PI as representative experimental groups. iC-PI and PEGDA/HEMA were used as controls. Degradation solutions with various dilutions and periodical release solutions were obtained using the same protocol as in the corresponding anti-bacterial study, using YM broth instead of tryptic soy/LB broth. Degradation products with different dilutions or periodical release solutions collected at different time points were put in the wells of 24-well tissue culture plates (450 μL per well), with blank YM broth samples as control. 50 μL of *C. albicans* suspension in Tween-20 containing YM broth medium was added to each well, with the initial fungi concentration kept in the range of $0.5–1 \times 10^7$ cells/mL. The 24-well plates were incubated at 37 °C for 3 h with shaking at 100 rpm. The resulting solution was diluted 300 times, and cast on YM agar plates. After incubation at 37 °C for 24 h, fungi colonies on the YM agar plates were counted, and the fungal survival ratios were calculated according to equation (5).

3. Results

3.1. Synthesis and characterization of anti-fungal iCMBA (AiC) pre-polymers

First, anti-fungal citric acid, 10-undecenoyl acid (UA) modified citric acid (U-CA), was synthesized through the reaction between dried citric acid (CA) and 10-undecenoyl chloride catalyzed by $ZnCl_2$ (Scheme 1A). Only the hydroxyl group on CA was modified in this reaction. The three carboxyl groups on CA were preserved for further reaction with poly(ethylene glycol) (PEG) and dopamine through a convenient one-pot polycondensation to give anti-fungal injectable citrate-based mussel-inspired bioadhesives pre-polymers (Anti-fungal iCMBAs, AiCs) (Scheme 1B). FTIR spectra of representative AiC and normal iCMBA (iC) pre-polymers are shown in Fig. 1A. The peak between 1700 and 1748 cm^{-1} was assigned to the carbonyl group (C═O) in the ester group and the peak around 1540 cm^{-1} was assigned to the amide group (−C(=O)−NH-). The peak around 2900 cm^{-1} was assigned to methylene groups from PEG and UA. Higher absorption for this peak in the FTIR spectrum of AiC was attributed to the incorporation of UA. The successful incorporation of UA was further confirmed by the appearance of peaks in the low ppm range (1–2 ppm) in the ^1H NMR spectrum of AiC, while no peaks in the same range were found in the spectrum of corresponding iC pre-polymer (Fig. 1B).

The dopamine content in all AiC and iC pre-polymers was determined by their absorptions at 280 nm wavelength according to the dopamine standard curve shown in Fig. 1C (results are presented in Table 1) under an UV–vis spectrophotometer. The UV–vis spectroscopy of representative AiC and iC pre-polymers are shown in Fig. 1D. iC-P_{200} showed the highest absorption at 280 nm, followed by AiC-P_{200}, AiC-P_{400}, AiC-P_{1000} and AiC-P_{4A800}. AiC-P_{3A1000} gave the lowest absorption. AiC-$P_{2/4(1/1)}$ synthesized using a PEG200 and PEG400 mixture (w/w = 1/1) was also obtained, and its dopamine content was determined to be 0.538 mmol/g, between that of AiC-P_{200} and AiC-P_{400} (Table 1).

3.2. Gelling time of AiCs

In this work, two oxidants, silver nitrate (SN) and sodium (meta) periodate (PI), were used to cross-link AiC into anti-bacterial and anti-fungal iCMBA (AbAf iC) bioadhesives. Gelling times of iC-P_{200} cross-linked by SN at different pH values are shown in Fig. 2A. iC-P_{200} solutions with higher pH values cross-linked faster. The gelling time at pH 8.5 was around 149 s, which was the shortest, and pre-polymer solution in DI water without pH adjustment (pH around 2.8) could not be cross-linked by SN. The gelling times of different AiC or iC pre-polymers cross-linked by different SN or PI amounts are shown in Fig. 2B and/or listed in Table 2. With the help of hydrophobic UA groups, the cross-linking of AiCs was faster than their iC pre-polymer counterparts. The measured gelling times of AiC pre-polymers ranged from 26 s for AiC-P_{4A800} SN 0.15 g/mL up to slightly over 3 min (193s) for AiC-P_{1000} SN 0.15 g/mL. Higher dopamine content in AiC decreased gelling time as did the use of 3- or 4-armed PEGs. AiC pre-polymer incorporating PEG with higher molecular weight exhibited longer gelling time. The gelling time of AiC-$P_{2/4(1/1)}$ PI 8 wt% was also measured to be 126 s. All gelling times were measured at room temperature (25 °C).

Table 2
Gelling time of different iCMBAs and anti-fungal iCMBAs cross-linked by various ratios of oxidants (silver nitrate, SN or sodium periodate, PI) under different pH values at room temperature (pre-polymer concentration was 50 wt% for all samples).

Pre-polymer name[a]	Oxidant concentration used (g/mL)	Oxidant to pre-polymer ratio (g/g polymer)[b]	Test pH value[c]	Measured gel time (s)
iC-P_{200}	SN 0.15	0.15	2.8	uncross-linkable
iC-P_{200}	SN 0.15	0.15	5	578
iC-P_{200}	SN 0.15	0.15	7	363
iC-P_{200}	SN 0.15	0.15	8.5	149
AiC-P_{200}	SN 0.10	0.1	8.5	99
AiC-P_{200}	SN 0.15	0.15	8.5	53
AiC-P_{400}	SN 0.15	0.15	8.5	85
AiC-P_{1000}	SN 0.15	0.15	8.5	193
AiC-P_{3A1000}	SN 0.15	0.15	8.5	48
AiC-P_{4A800}	SN 0.15	0.15	8.5	26
AiC-$P_{2/4\ (1/1)}$	SN 0.15	0.15	8.5	66[e]
AiC-$P_{2/4\ (1/1)}$	PI 8 wt%	8 wt% to polymer	As it[d]	126[e]

[a] For the ones cross-linked by silver nitrate (SN), pre-polymers were dissolved in 0.1 M Tris-HNO_3 (pH 13) buffer with a concentration of 50 wt%; for those cross-linked by sodium periodate (PI), pre-polymer was dissolved in DI water with a 50 wt% concentration.
[b] Silver nitrate (SN) used was dissolved in 0.1 M Tris-HNO_3 (pH 8.5) buffer, while sodium periodate (PI) was dissolved in DI water.
[c] For the ones cross-linked by SN, the tested pH values were adjusted using 12 M NaOH and 70% nitric acid.
[d] Pre-polymer was dissolved in DI water (50 wt%) and used as is.
[e] Obtained by vial tilting method.

3.3. Properties of cross-linked AbAf iCs

Mechanical properties of cross-linked AbAf iCs in dry and fully hydrated states are tabulated in Table S1. In the dry state, the highest tensile strength, elongation at break, and Young's modulus were 3312.3 ± 495 kPa (AiC-P_{200} SN 0.15 g/mL), 415.6 ± 87.52% (AiC-P_{400} SN 0.15 g/mL), and 51561 ± 7712 kPa (AiC-P_{200} SN 0.15 g/mL), respectively. The stress–strain curves of cross-linked AbAf iCs are also shown in Fig. 3A. All AbAf iCs demonstrated an elastomer behavior, except iC-P_{200} SN 0.15 g/mL. The mechanical strength decreased when samples were hydrated and swollen, which is attributed to the hydrophilicity of AbAf iCs derived from hydrophilic PEG.

The degradation studies of dried hydrogels revealed that the degradation rate was inversely related to the degree of cross-linking and the amount of hydrophobic UA. As shown in Fig. 3B, for the hydrogels cross-linked by SN, AiC-P_{200} SN 0.15 g/mL exhibited the slowest degradation, with complete degradation in 23 days in PBS at 37 °C, while AiC-P_{1000} SN 0.15 g/mL exhibited the fastest degradation, with nearly 90 wt% mass loss in one day. Hydrogels cross-linked with PI degraded slower, due to the lower cross-linking degree of hydrogels cross-linked by SN compared to those cross-linked by PI. It is probable that after SN was reduced into silver nanoparticles, the oxidized catechol groups on AiCs were partially used for silver nanoparticle chelation rather than cross-linking between each other (Scheme S1). The long gelling time (around 30 min) of similar dopamine containing polymers cross-linked by silver nitrate supports this theory [25].

Sol contents of different AbAf iCs cross-linked by SN or PI are shown in Fig. 3C. For the hydrogels cross-linked by SN, AiC-P_{200} SN 0.15 g/mL possessed the lowest sol content, which is much lower than that of iC-P_{200} SN 0.15 g/mL which contains no hydrophobic UA. AiC-P_{1000} SN 0.15 g/mL exhibited the highest sol content of around 37%. AiC-$P_{2/4(1/1)}$ PI 8wt% (7.31%) possessed much lower sol content than that of AiC-$P_{2/4(1/1)}$ SN 0.15 g/mL (18.27%), and the sol contents of AiCs cross-linked by SN are even higher than that of iCMBA counterparts (containing no hydrophobic UA) cross-linked by PI [18], which further confirmed that hydrogels cross-linked by SN possess a lower cross-linking degree than those cross-linked by PI. Partial degradation in the process of pH adjustment to 8.5 before cross-linking may be another reason for this trend. The swelling ratio data shows that for hydrogels cross-linked by SN, AiC-P_{200} SN 0.15 g/mL, which has the highest dopamine content and the smallest molecular weight of PEG, possessed the lowest swelling ratio of around 347.5% as shown by Fig. 3D. On the other hand, AiC-P_{1000} SN 0.15 g/mL displayed the highest swelling ratio of around 1692.4%. AiC-$P_{2/4(1/1)}$ PI 8wt% (167.9%) also possessed a much lower swelling ratio that of AiC-$P_{2/4(1/1)}$ SN 0.15 g/mL (515.1%), which further confirmed that hydrogels cross-linked by SN possess a lower cross-linking degree.

3.4. Adhesion strength

The wet lap shear strength of different AbAf iC formulations varied between 32.85 ± 7.03 kPa (for AiC-P_{400} SN 0.15 g/mL) and 168.15 ± 17.02 kPa (for AiC-P_{1000} PI 8 wt%). Although the adhesion strengths of bioadhesives cross-linked by SN were much lower than that of bioadhesives cross-linked by PI, the adhesion strengths were still higher than that of gold standard, commercially available fibrin glue (15.4 ± 2.8 kPa) [18], as shown in Fig. 4 and Table S2.

3.5. In vitro cell cytotoxicity and proliferation

The results of cell cytotoxicity of AiC pre-polymers are shown in Fig. 5A. At the concentration of 10 mg/mL (in cell culture medium), the cell viabilities of all AiC pre-polymers against hMSCs were between 56.7 ± 2.04 and 66.5 ± 4.30%, comparable to the value for the control (PEGDA 700) of 57.1 ± 1.63%, and there were no significant differences between different pre-polymers. In diluted AiC pre-polymers solutions of 1 and 0.1 mg/mL, the cell viabilities were similar to that of blank medium and PEGDA. Although the cell viabilities of the leachable contents (sol contents) of cross-linked AbAf iCs at 1 × concentration were all around 10% or even lower, the cell viabilities of sol contents at 10 × were all higher than 80%, and all higher than 90% at 100 × concentration. The cytotoxicity of cross-linked AbAf iCs' sol contents is considered to be a result of the formed silver nanoparticles or excess PI (Fig. 5B). Although AbAf iCs degradation products at 1 × concentration also exhibited higher cytotoxicities (lower than 40%) compared to that of PLGA (~80%), a widely used FDA-approved commercially available biodegradable polymer, the diluted solutions of AbAf iCs degradation products at 10 × and 100 × were all higher than 90%, and comparable to that of blank medium and PLGA (Fig. 5C), further indicating the low cytotoxicity of cross-linked AbAf iCs. The proliferation of hMSCs on cross-linked AbAf iCs films was also investigated by Live/Dead assay over three time points (1, 3, and 7 days) (Fig. 5D). The stretched cell

morphology of hMSCs indicated good cell attachment and proliferation on cross-linked AbAf iCs films.

3.6. Anti-bacterial performance of AbAf iCs

The bacterial inhibition ratios of AbAf iCs, cross-linked by either PI or SN, against *S. aureus* were all higher than 90% after 4 h incubation of 0.2 g dried hydrogel in 20 mL bacteria suspension (initial OD_{600nm}—0.1) (Fig. 6A). High inhibition ratios (>90%) were kept even after 24 h. In addition to AiC-SN, the bacterial inhibition ratios of AiC-PI and iC-PI for all time points were also all higher than 90%, indicating that PI cross-linked bioadhesives also exhibited very good *S. aureus* inhibition. The bacterial inhibition ratios of PI solution (8 wt%) against *S. aureus* were all higher than 100% during the 24 h of incubation (Fig. 6A). The *S. aureus* inhibition ratios of 29 mg/mL CA were also all around 100% during 2—24 h in the incubation process. The control sample, PEGDA/HEMA, exhibited no inhibition against *S. aureus* in the whole 24 h' incubation process.

Although the inhibition ratios of AbAf iCs (cross-linked either by PI or SN) against *E. coli* were not as high as that against *S. aureus*, more that 80% of *E. coli* were inhibited at all time points during 6—24 h (Fig. 6B). The *E. coli* inhibition ratios of iC-PI were also lower than that against *S. aureus*, indicating that the inhibition effect of PI against *E. coli* was weaker than against *S. aureus*, which also can be seen from the *E. coli* incubation test using 8 wt% PI (Fig. 6B). The *E. coli* inhibition ratios of 29 mg/mL of CA were all around 95%, lower than that against *S. aureus*, which is in agreement with our previous work [20]. The control sample, PEGDA/HEMA, also exhibited no inhibition against *E. coli*. The image of bacteria in broth media before and after incubation with AbAf iCs, iC-PI, CA (29 mg/mL), and PI (8 wt%) for 24 h is show in Fig. 6C. The bacterial inhibition effect could be visually observed by the clarity of the symbol "PSU" on a paper underneath the 96-well plate.

The inhibition halos of AbAf iCs against *S. aureus* and *E. coli* are shown in Fig. 6D. After 24 h' incubation at 37 °C, both AiC-PI and AiC-SN clearly showed anti-bacterial halos against *S. aureus* and *E. coli*. The zones of inhibition were 28.5, 32.0 mm (*S. aureus*) and 14.0, 21.5 mm (*E. coli*) respectively. The zones of inhibition of iC-PI against *S. aureus* and *E. coli* were 31.0 and 20.5 mm respectively. The control sample, PEGDA/HEMA, exhibited only very weak inhibition against the two kinds of bacteria.

3.7. Anti-fungal performance of AbAf iCs

The fungal survival ratios after direct exposure to AiC-PI, AiC-SN, or iC-PI for 3 h were 0.14, 8.29, and 4.89% respectively, while PEGDA/HEMA showed very weak inhibition against the fungi used, *C. albicans* (Fig. 7A). The zones of inhibition of AiC-PI, AiC-SN, and iC-PI against *C. albicans* were measured to be 55.8, 31.1, and 37.9 mm respectively, while PEGDA/HEMA showed no inhibition zone (Fig. 7B).

3.8. Long-term anti-bacterial and anti-fungal performance of AbAf iCs

From Fig. 8A, it can be seen that the 1 × degradation solutions of

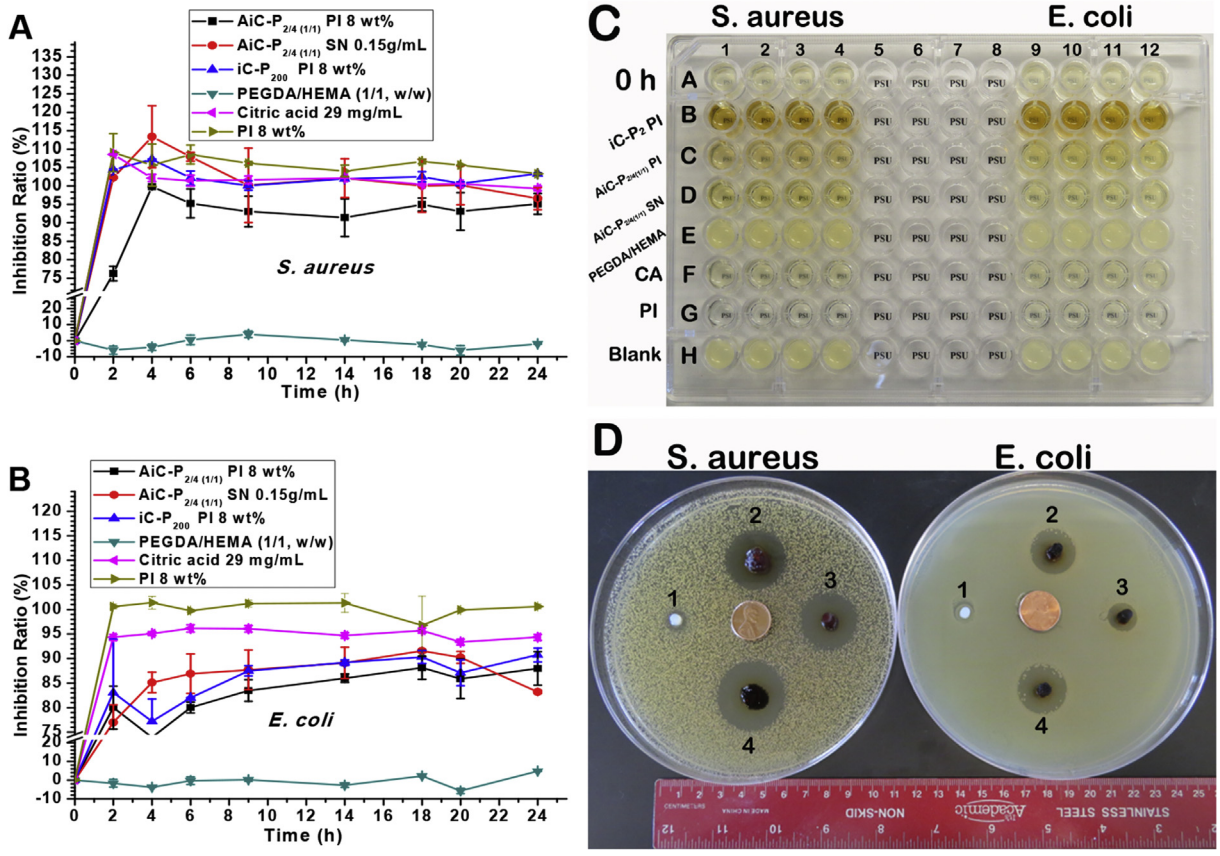

Fig. 6. Anti-bacterial performance of AbAf iCMBAs: Inhibition ratios kinetics curves of cross-linked AbAf iCMBAs, iC-P_{200} PI 8 wt%, PEGDA/HEMA (w/w = 1/1, as conrol), and citric acid (CA, 29 g/mL) as well as sodium periodate (PI, 8 wt%) against S. aureus (A) and E. coli. (B). Image of bacteria in broth media before and after being directly exposed to cross-linked AbAf iCMBAs, CA (29 mg/mL) and PI (8 wt%) for 24 h (C), the 96-well plate was placed on a piece of paper with one "PSU" symbol underneath each well. Inhibition halos of cross-linked hydrogels after 24 h incubation at 37 °C (D), 1. PEGDA/HEMA (w/w = 1/1), 2. iC-P_{200} PI 8 wt%, 3. AiC-$P_{2/4(1/1)}$ PI 8 wt%, and 4. AiC-$P_{2/4(1/1)}$ SN 0.15 g/mL.

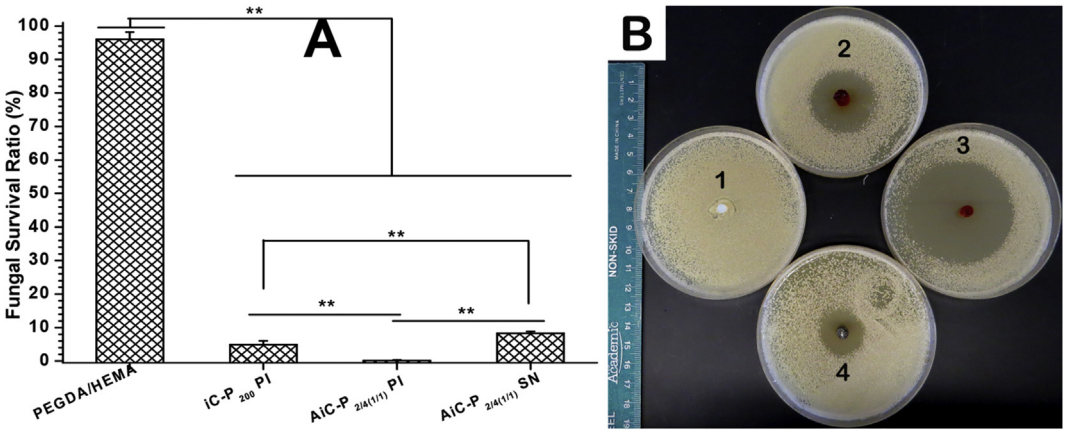

Fig. 7. Anti-fungal performance of AbAf iCMBAs against C. albicans: Fungal survival ratios after direct exposure to cross-linked AbAf iCMBAs, iC-P_{200} PI 8 wt%, and PEGDA/HEMA (w/w = 1/1, as control) for 3 h (A) (**p < 0.01). Inhibition halos of cross-linked hydrogels to C. albicans after incubation at 37 °C for 24 h (B), 1. PEGDA/HEMA (w/w = 1/1), 2. iC-P_{200} PI 8 wt%, 3. AiC-$P_{2/4(1/1)}$ PI 8 wt%, and 4. AiC-$P_{2/4(1/1)}$ SN 0.15 g/mL.

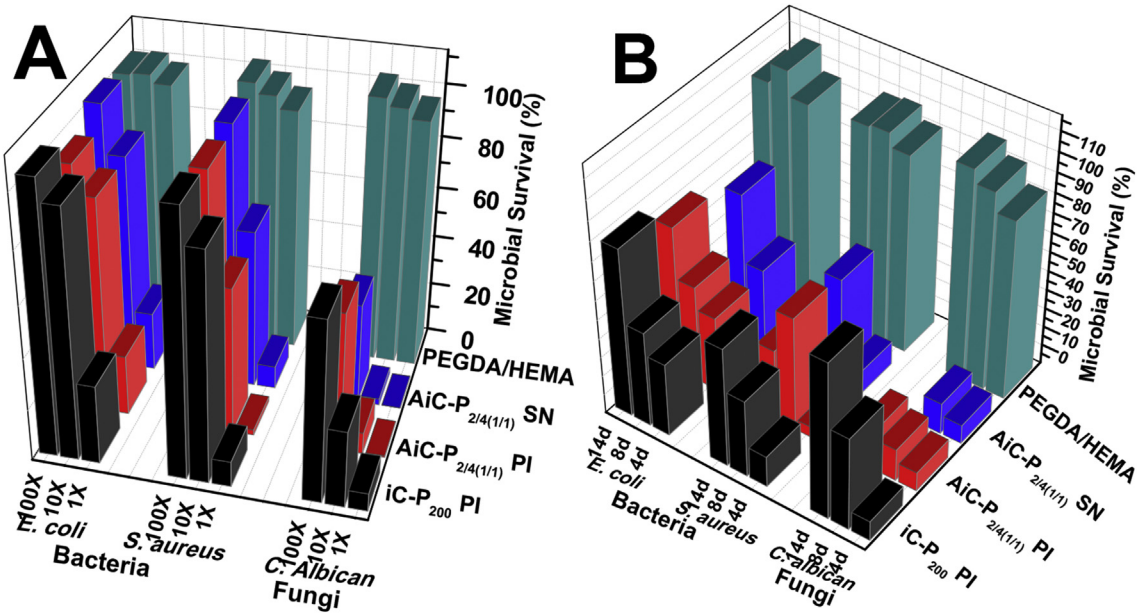

Fig. 8. Long-term anti-microbial study: Anti-fungal and anti-bacterial performance of degradation products (A) and release solutions (B) of cross-linked hydrogels: iC-P_{200} PI 8 wt%, AiC-$P_{2/4(1/1)}$ PI 8 wt%, AiC-$P_{2/4(1/1)}$ SN 0.15 g/mL and PEGDA/HEMA (w/w = 1/1, as control).

AiC-PI, AiC-SN, and iC-PI exhibited very good zone of inhibition (survival ratios < 10%) against *C. albicans* (fungi) and *S. aureus* (Gram-positive bacteria), but exhibited weaker inhibition (survival ratios ~20%) against *E. coli* (Gram-negative bacteria). The 10 × diluted degradation solutions of AiC-PI and AiC-SN still showed considerable anti-fungal properties but much weaker inhibition against both *S. aureus* and *E. coli*. Containing no UA, the 10 × diluted degradation solution of iC-PI exhibited much weaker fungal inhibition compared to that of AiC-PI and AiC-SN, and also exhibited very weak bacterial inhibition. The degradation solutions of PEGDA/HEMA at all diluted concentrations exhibited very weak fungal and bacterial inhibition.

From the results of microbial survival ratios of microbes incubated with periodical release solutions of AbAf iCs shown in Fig. 8B, it can be seen that the 4th day's release solutions of AiC-PI, AiC-SN, and iC-PI all exhibited very favorable inhibition (survival ratios < or ~5%) against *C. albicans* (fungi) and *S. aureus* (Gram-positive bacteria), but exhibited a much weaker inhibition (survival ratios ~ 30%) against *E. coli* (Gram-negative bacteria). The 8th day's release solutions of AiC-PI, AiC-SN, and iC-PI could inhibit 60–70% bacteria for both *S. aureus* and *E. coli*. The 8th day's release solutions of AiC-PI and AiC-SN exhibited much better fungal inhibition (with survival ratios of 6.79 and 6.31% respectively) compared to that of iC-PI (38.8%). The 12th day's release solution of AiC-PI still exhibited a fungal inhibition ratio around 88%, which is much higher than that of iC-PI (inhibition ratio = 28.2%), while AiC-SN broke up into small pieces after 8 days of incubation in PBS (pH 7.4) at 37 °C. The bacterial survival ratios of the 12th day's release solutions were overall higher than that of the 8th day's solutions, except that of AiC-PI against *S. aureus*. The release solutions of PEGDA/HEMA at all three time points exhibited nearly no bacterial or fungal inhibition.

4. Discussion

Anti-fungal iCMBAs (AiCs) were synthesized in two steps (Scheme 1). First, anti-fungal citric acid (undecylenate citric acid, U-

CA) was synthesized through the reaction between the –OH groups on citric acid (CA) and 10-undecenoyl chloride catalyzed by $ZnCl_2$ (Scheme 1A). Then U-CA was used to synthesize AiCs together with CA, PEG, and dopamine through a single-step, catalyst-free, one-pot polycondensation process (Scheme 1B). The successful incorporation of U-CA was confirmed by FTIR and ^{1}H-NMR characterization (Fig. 1A, B).

UV–vis photospectroscopy confirmed the availability of unoxidized catechol hydroxyl groups in all AiC pre-polymers through the observation of UV absorption at 280 nm in all samples (Fig. 1D). The oxidization of catechol groups into quinone groups could be verified by UV–vis absorption of quinone at around 390 nm [29]. The presence of unoxidized catechol groups is essential for adhesion and the cross-linking process [18]. The dopamine (catechol group) contents of AiC pre-polymers were also quantitatively determined by the UV absorption of pre-polymer at 280 nm according to the dopamine standard curve shown in Fig. 1C (results are shown in Table 1). The dopamine contents of AiC pre-polymers with high molecular weight and star shaped PEGs (PEG 1000, 3A1000 and 4A800) were lower than expected, which can be attributed to the possible partial oxidization of catechol groups due to longer reaction time (for pre-polymer with PEG1000), or to the lowered dopamine reactivity caused by the larger steric hindrance of branched PEG (for pre-polymer with PEG 3A1000 or 4A800).

Two kinds of oxidants, sodium periodate (PI) and silver nitrate (SN), were used to cross-link AiCs (Scheme S1). Because the gelling times of iCMBAs (iCs, not containing UA) cross-linked by PI were thoroughly studied in our previous work [15], in this paper we focused on the investigation of gelling times of AiCs cross-linked by SN. When SN was used as the cross-linking initiator, the gelling times of iC-P_{200} were greatly related to the pH value of iC-P_{200} solutions, with higher pH values leading to faster cross-linking. The gel time at pH 8.5 (149s) was significantly shorter than that at pH 5 (578s), and the iC-P_{200} solution without pH adjustment (pH~2.8) could not be cross-linked by SN (Fig. 2A). The gel times of AiC pre-polymers cross-linked by 0.15 g/mL SN at pH 8.5 were in the range of 26–193 s. The incorporation of hydrophobic UA molecules, increase of SN concentration, and usage of shorter chain or branched PEG could decrease the gelling times (Fig. 2B and Table 2). Although the cross-linking of AiCs by SN at pH 8.5 was faster than that of iCMBAs cross-linked by PI, and the incorporation of hydrophobic UA improved the hydrophobicity of the pre-polymer, the cross-link density of AiCs cross-linked by SN seems lower than that of iCMBAs cross-linked by PI, which is supported by the sol content and swelling ratio data (Fig. 4C, D). The high sol contents and swelling ratios were attributed to the chelating effects of the generated silver nanoparticles to unoxidized and oxidized (quinone) catechol groups, which prevented the oxidizing of catechol groups and cross-linking between quinone groups (Scheme S1). Partial degradation of AiC caused by high pH value may also contribute to the decreased cross-link density. When PI was used as the cross-linking initiator for AiC, the sol content and swelling ratio were significantly reduced compared with the same pre-polymer cross-linked by SN (Fig. 3C, D).

The study of mechanical properties of cross-linked AbAf iCs suggested that these materials demonstrated elastomeric behavior with typical stress–strain curves of elastomers (Fig. 3A and Table S1), which is very important for their application as soft tissue adhesives which resemble the elastic nature of soft tissues. Tensile strength, elongation at break and modulus of AbAf iCs varied with the molecular weight and architecture of PEG and degree of cross-linking. The mechanical properties can be easily tuned as needed.

The degradation study revealed the fast degradation (complete degradation in one month) of all AbAf iCs, which not only leaves space for tissue regeneration, but also allows anti-fungal UA to be released from the cross-linked polymer (Fig. 3B). The degradation times of AbAf iCs were not much longer compared to pure iCMBAs that contain no UA, as expected [18], which further proved that the cross-link density of AiCs cross-linked by SN is lower than that of iCMBAs cross-linked by PI. When PI was used for cross-linking, the degradation time was prolonged considerably compared to that of corresponding iCMBA (Fig. 3B).

Under the help of hydrophobic UA, when the same amount of PI was used as cross-linking initiator, the wet tissue bonding strengths of AbAf iCs measured by the lap shear strength tests, as shown in Fig. 4 and Table S2 (highest was 168.15 ± 17.02 kPa), were higher than those of corresponding pure iCMBAs [18]. Although when SN was used as cross-linking initiator the lap shear strengths of Abaf iCs decreased, the values were still higher than that of gold standard fibrin glue, a clinically used commercially available bioadhesive.

The quantitative *in vitro* cell cytotoxicity evaluations of AiC pre-polymers, sol contents, and degradation products of cross-linked AbAf iCs revealed that although the formed silver nanoparticles possess certain cytotoxicity, after dilution the tested formulas did not induce significant cytotoxicity to hMSCs (Fig. 5A–C). These results along with qualitative cell proliferation and morphology observation (Fig. 5D) demonstrated that AbAf iCs are potentially excellent candidates for biological and biomedical applications.

The anti-bacterial studies showed that the tested AbAf iCs cross-linked by either SN or PI both exhibited excellent bacterial inhibition performance against both *S. Aureus* and *E. coli* during 24 h of incubation when bacteria were directly exposed to the hydrogels (Fig. 6). Silver nanoparticles have been widely used as an anti-bacterial agent for a long time [6,23,25], and should play an important role in the bacterial inhibition of AiC-$P_{2/4(1/1)}$ SN 0.15 g/mL (abbreviated as AiC-SN). AiC or iC pre-polymers cross-linked by PI exhibited similar or even better anti-bacterial performance, which was unexpected. To investigate the anti-bacterial ability of iC-P_{200} PI 8wt% (iC-PI) and AiC-$P_{2/4(1/1)}D_{0.3}$ PI 8wt% (AiC-PI), the anti-bacterial properties of the components of these polymers, including citric acid (CA), PI, and UA, were thoroughly investigated, (results are shown in Fig. S1). CA, PI and UA all exhibited better inhibition against *S. aureus* than against *E. coli* (Fig. S1A, E, H). The minimal inhibitory concentrations (MICs) of CA, PI, and UA against *S. aureus* or *E. coli* were around 8 and 8 mg/mL (CA), 0.0556 and 0.222 wt% (PI), and 0.5, - mg/mL (UA had no inhibition against *E. coli.* in the tested concentration range), respectively. Without having UA, iC-PI still exhibited very good anti-bacterial performances, leading to the conclusion that UA is not the only anti-bacterial component (Scheme S1). Although CA exhibited certain anti-bacterial ability against both *S. aureus* and *E. coli,* after being buffered (pH adjusted to 7.4) its bacterial inhibition ability became much weaker, especially for *E. coli.* Buffered CA with a concentration up to 58 mg/mL could only inhibit 31.58% of *E. coli* (Fig. S1B). PI exhibited the best anti-bacterial properties among the three tested components. In the crosslinking process of iCMBAs, PI should be reduced into $NaIO_3$ or even I_2, both of them are often clinically used as antimicrobial agents (Scheme S1). The residual PI and its reduced components are also small molecules that could be easily released from the hydrogel, which was deemed to play the most important role in the strong initial bacterial inhibition performance of AbAf iCs and normal iCMBAs cross-linked by PI (Scheme S1). Although PI is often used as an anti-microbial agent in aquaculture, the application of PI as an anti-bacterial agent in the biomedical field is rarely mentioned. Thus the cytotoxicity of PI against hMSCs was investigated. The results as shown in Fig. S1G indicated that at low concentrations, PI induced no significant cytotoxicity but still preserved comparative inhibition to bacteria. Cytotoxicity evaluation of CA confirmed its biocompatibility (Fig. S1D).

The fungal inhibition evaluation suggested that the tested AbAf iCs cross-linked by either SN or PI both exhibited even better anti-fungal performance against *C. albicans* than their anti-bacterial performance (Fig. 7). Polymers with anti-fungal UA segments and/or cross-linked by PI exhibited better antifungal ability than others, with AiC-PI that contains UA and was cross-linked by PI exhibiting the best antifungal ability. The anti-fungal performance of the components of AbAf iCs, containing CA, PI, and UA, were also evaluated (results are shown in Fig. S1A–I). Both CA and buffered CA exhibited weak anti-fungal ability. The MICs of CA and buffered CA against *C. albicans* were all around 58 mg/mL (Fig. S1A, B). The images of the anti-fungal test of CA and buffered CA are shown in Fig. S1C. PI exhibited very good fungal inhibition against *C. albicans*, with a MIC of 0.0139 wt%, which is even lower than that against *S. aureus* (Fig. S1E). The image of the anti-fungal test for PI is shown in Fig. S1F. UA is a widely used anti-fungal agent, with the MIC of UA against *C. albicans* determined to be 0.25 mg/mL (Fig. S1E, F), which is in agreement with the previously reported data [30]. The anti-fungal test of AiC-$P_{2/4(1/1)}$ and iC-P_{200} pre-polymers against *C. albicans* indicated that AiC-$P_{2/4(1/1)}$ containing UA segments exhibited better anti-fungal performance than the pre-polymer containing no UA (Fig. S1I). The above studies indicated that PI, silver nanoparticles, and UA all played important roles in the initial anti-fungal performance of AbAf iCs (Scheme S1).

Long-term anti-bacterial and anti-fungal performance of AbAf iCs was investigated by measuring the microbial survival ratios after incubating bacteria and fungi with the degradation products (1 ×, 10 ×, and 100 × of dilutions) and the release solutions (4, 8, and 12 days) of AbAf iCs for 24 (for bacteria) or 6 (for fungi) hrs (results are shown in Fig. 8). The results revealed that AiC-SN, AiC-PI, and iC-PI all exhibited considerable long-term inhibition against bacteria and fungi, especially against Gram-positive bacteria *S. aureus* and fungi (Fig. 8A, B). This phenomenon is in agreement with the above initial anti-bacterial and anti-fungal results and the fact that all three components, CA, PI, and UA, exhibited better inhibition against *S. aureus* and fungi than *E. coli*. AiC-PI and AiC-SN that contain anti-fungal UA exhibited better long-term inhibition against fungi than iC-PI, especially at the time points of the 8th and the 12th days. The unreacted PI or the silver nanoparticles were most likely leached out from the hydrogels in the first 4 days. UA was thus considered to play the most important role in long-term anti-fungal behavior (Fig. 8B). Although AiC-SN and AiC-PI exhibited comparable anti-fungal performance in the beginning, AiC-SN degraded faster than AiC-PI, and the swelling ratio of AiC-SN was much higher than that of AiC-PI. AiC-PI is considered a better candidate for anti-bacterial and anti-fungal bioadhesive.

5. Conclusion

Through the introduction of the clinically used and inexpensive anti-fungal agent, 10-undecylenic acid (UA), into our recently developed injectable citrate-based mussel-inspired bioadhesives (iCMBAs), a new family of anti-bacterial and anti-fungal iCMBAs (AbAf iCs) was developed for applications in tissue/wound closure, wound dressing, and bone regeneration. The anti-bacterial and anti-fungal performance and the biocompatibility of AbAf iCs as well as their components, citric acid (CA), sodium metaperiodate (PI, an oxidant, used as cross-linking initiator), and UA, were systematically studied. AbAf iCs exhibited strong initial inhibition of bacteria and fungi by the burst release of PI/silver nanoparticles, and long-term anti-fungal performance when anti-fungal UA was degraded from the bioadhesives. PI cross-linked bioadhesives were found to exhibit even better anti-microbial ability than the silver-based bioadhesives. The development of AbAf iCs expands our bioadhesives family with anti-microbial and anti-fungal properties that may be essential for many biomedical applications such as wound closure, wound dressing, and bone regeneration, particularly where bacterial and/or fungal infection is prevalent.

Acknowledgments

This work was supported in part by National Institutes of Health awards (EB012575, CA182670, HL118498) and National Science Foundation (NSF) awards (DMR1313553, CMMI1266116, CMMI1537008).

Appendix A. Supplementary data

Supplementary data related to this article can be found at http://dx.doi.org/10.1016/j.biomaterials.2016.01.069.

References

[1] M.C. Giano, S.H. Medina, K.A. Sarhane, J.M. Christensen, Y. Yamada, G. Brandacher, J.P. Scheneider, Injectable bioadhesive hydrogels with innate antibacterial properties, Nat. Commun. (2014), http://dx.doi.org/10.1038/ncomms5095.
[2] I. Manolakis, B.A.J. Nooedover, R. Vendamme, W. Eevers, Novel L-DOPA-derived poly(ester amide)s: monomers, polymers, and the first L-DOPA functionalized biobased adhesive tape, Macromol. Rapid Commun. 35 (2014) 71–76.
[3] M. Mehdizadeh, J. Yang, Design strategies and applications of tissue bioadhesives, Macromol. Biosci. 13 (2013) 271–288.
[4] L.I.F. Moura, A.M.A. Dias, E. Carvalho, H.C. de Sousa, Recent advances on the development of wound dressings for diabetic foot ulcer treatment—A review, Acta Biomater. 9 (2013) 7093–7114.
[5] H. Brem, M. Tomic-Canic, Cellular and molecular basis of wound healing in diabetes, J. Clin. Invest. 117 (2007) 1219–1222.
[6] Y. Zhou, Y. Zhao, L. Wang, L. Xu, Z. Zhai, S. Wei, Radiation synthesis and characterization of nanosilver/gelatin/carboxymethylchitosan hydrogel, Radiat. Phys. Chem. 81 (2012) 553–560.
[7] S.P. Hudson, R. Langer, G.R. Fink, D.S. Kohane, Injectable in situ cross-linking hydrogels for local antifungal therapy, Biomaterials 31 (2010) 1444–1452.
[8] J. Yang, A.R. Webb, G.A. Ameer, Novel citric acid-based biodegradable elastomers for tissue engineering, Adv. Mater. 16 (2004) 511–516.
[9] R.T. Tran, J. Yang, G.A. Ameer, Citrate-based biomaterials and their applications in regenerative engineering, Annu. Rev. Mater. Res. 45 (2015) 277–310.
[10] J. Yang, Y. Zhang, S. Guntam, L. Liu, J. Dey, W. Chen, et al., Development of aliphatic biodegradable photoluminescent polymers, Proc. Natl. Acad. Sci. U. S. A. 106 (2009) 10086–10091.
[11] J. Guo, Z. Xie, R.T. Tran, D. Xie, D. Jin, X. Bai, J. Yang, Click chemistry plays a dual role in biodegradable polymer design, Adv. Mater. 26 (2014) 1906–1911.
[12] Z. Xie, Y. Zhang, L. Liu, H. Weng, R.P. Mason, L. Tang, et al., Development of intrinsically photoluminescent and photostable polylactones, Adv. Mater. 26 (2014) 4491–4496.
[13] J. Hu, J. Guo, Z. Xie, D. Shan, E. Gerhard, G. Qian, J. Yang, Fluorescence imaging enabled poly(Lactide-co-glycolide), Acta Biomater. 29 (2016) 307–319.
[14] D. Sun, Y. Chen, R.T. Tran, S. Xu, D. Xie, C. Jia, et al., Citric acid-based osteoinductive scaffolds enhance calvarial regeneration, Sci. Rep. 4 (2014) 6912.
[15] D. Xie, J. Guo, M. Mehdizadeh, R.T. Tran, R. Chen, D. Sun, et al., Development of injectable citrate-based bioadhesive bone implants, J. Mater. Chem. B 3 (2015) 387–398.
[16] J. Tang, J. Guo, Z. Li, C. Yang, J. Chen, S. Li, et al., A fast degradable citrate-based bone scaffolds promotes spinal fusion, J. Mater. Chem. B 3 (2015) 5569–5576.
[17] L.C. Su, H. Xu, R.T. Tran, Y.T. Tsai, L. Tang, J. Yang, K.T. Nguyen, In-situ reendothelialization via multifunctional nano-scaffolds, ACS Nano 8 (2014) 10826–10836.
[18] M. Mehdizadeh, H. Weng, D. Gyawali, L. Tang, J. Yang, Injectable citrate-based mussel-inspired tissue bioadhesives with high wet strength for sutureless wound closure, Biomaterials 33 (2012) 7972–7983.
[19] B.P. Lee, J.L. Dalsin, P.B. Messersmith, Synthesis and gelation of DOPA-modified poly(ethylene glycol) hydrogels, Biomacromolecules 3 (2002) 1038–1047.
[20] H.J. Kim, B.H. Hwang, S. Lim, B.-H. Choi, S.H. Kang, H.J. Cha, Biomaterials 72 (2015) 104–111.
[21] R.K. Pundir, P. Jain, Evaluation of five chemical food preservatives for their antibacterial activity against bacterial isolates from bakery products and mango pickles, J. Chem. Pharm. Res. 3 (2011) 24–31.
[22] L.C. Su, Z. Xie, Y. Zhang, K.T. Nguyen, J. Yang, Study on the antimicrobial properties of citrate-based biodegradable polymers, Front. Bioeng. Biotechnol. 2 (2014) 23.
[23] H. Yu, X. Xu, X. Chen, T. Lu, P. Zhang, X. Jing, Preparation and antibacterial effects of PVA-PVP hydrogels containing silver nanoparticles, J. Appl. Polym.

Sci. 103 (2007) 125–133.
[24] M. Liong, B. France, K.A. Bradley, J.I. Zink, Antimicrobial activity of silver nanocrystals encapsulated in mesoporous silica nanoparticles, Adv. Mater. 21 (2009) 1684–1689.
[25] D.E. Fullenkamp, J.G. Rivera, Y.K. Gong, K.H.A. Lau, L.L. He, R. Varshney, P.B. Messersmith, Mussel-inspired silver-releasing antibacterial hydrogels, Biomaterials 33 (2012) 3783–3791.
[26] L. Tian, L. Yam, N. Zhou, H. Tat, K.E. Uhrich, Amphiphilic scorpion-like macromolecules: Design, synthesis, and characterization, Macromolecules 27 (2004) 538–543.
[27] D. Gyawali, P. Nair, Y. Zhang, R.T. Tran, C. Zhang, M. Samchukov, et al., Citric acid-derived in situ crosslinkable biodegradable polymers for cell delivery, Biomaterials 31 (2010) 9092–9105.
[28] D. Law, C.B. Moore, D.W. Denning, Amphotericin B resistance testing of Candida spp.: a comparison of methods, J. Antimicrob. Chemother. 40 (1997) 109–112.
[29] D.G. Graham, P.W. Jeffs, The role of 2, 4, 5-trihydroxyphenylalanine in melanin biosynthesis, J. Biol. Chem. 252 (1977) 5729–5734.
[30] L.M. Gonçalves, A.A. Del Bel Cury, A. Sartoratto, V.L. Garcia Rehder, W.J. Silva, Effects of undecylenic acid released from denture liner on candida biofilms, J. Dent. Res. 91 (2012) 985–989.